The Theory of Precipitation/Dissolution Waves

The concepts of coherence and composition paths, originally developed for multicomponent chromatography, are used to establish a simple theory of transport in systems with precipitation and dissolution in the course of multicomponent, single-phase flow in permeable media. Composition route construction in phase diagrams in combination with distance-time diagrams yields concentration profiles without recourse to trial-and-error procedures. Detailed results are given for systems with three ions *A*, *B*, and *X* and up to two precipitates *AX* and *BX*. The extension to systems with additional, nonprecipitating species is described. The new approach confirms most conclusions of Bryant's earlier theory, removes assumptions stipulated in the latter, and is simpler to handle.

Friedrich G. Helfferich
Department of Chemical Engineering
Pennsylvania State University
University Park, PA 16802

Introduction

An interesting and important class of phenomena in flow through permeable media involves precipitation and dissolution of sparingly soluble inorganic mineral salts. In essence, a precipitate is dissolved and its ions start to move with the fluid when an unsaturated fluid flows over it; it is deposited from the fluid when concentration variations let the solubility product be exceeded. Such processes are occasionally called metasomatic. Practical examples are found in leach mining (Tatom et al., 1981; Gao et al., 1981) and transport of metals in aquifers (Korzhinskii, 1970; Adler, 1974; Griffin et al., 1977; Galloway, 1982; Walsh et al., 1984; Dria et al., 1987). Another problem that may include this phenomenon in some cases is movement of contaminants in soils after discharge or spill (Hahne and Kroontje, 1973; Bartlett and Kimble, 1974; Bartlett and James, 1979; Khalid, 1980; Stohs, 1986).

Several theories for such systems have recently been developed. A finite-difference approach has been presented by Miller and Benson (1983). The most notable fundamental theories are by Klein (1986) and Bryant et al. (1986, 1987; Dria et al., 1987). Klein's theory is for ion-exchange columns in which salts such as calcium carbonate or sulfate may precipitate and dissolve in the course of operation. In its published version it is confined to binary ion exchange and a single precipitate, which may remain stationary or move with the fluid at its velocity. Bryant's complete theory (Bryant, 1986; Bryant et al., 1986; Dria et al., 1987), building on two basic postulates, is general in that it allows for ion exchange, adsorption, reactions in the fluid phase, and any number of components and precipitates and permits the latter to remain stationary or move with the fluid. However, in its general form this theory is difficult to apply. A simpler version (Bryant et al., 1987), excluding ion exchange, adsorption, fluid-phase reactions, and moving precipitate, alleviates this problem but still calls for trial-and-error searches. All applications published to date have been confined to the so-called Riemann problem (that is, to uniform initial and constant input conditions) or cases that can be compiled from several separate Riemann-problem solutions (Dria et al., 1987).

Both Klein and Bryant borrow from chromatography theory the concept of waves (that is, traveling concentration variations) and some of the tools, such as distance-time diagrams. Neither proceeds to apply other, well-developed concepts of multicomponent chromatography theory such as composition paths (Helfferich, 1968, 1984, 1988; Helfferich and Klein, 1970), Klein because his restriction to binary ion exchange makes this unnecessary, Bryant because of the fundamental difficulty that precipitation/dissolution systems do not provide continuous differentiable relations between the concentrations in the two phases. The purpose of the discussion to follow is to show that these concepts can indeed be applied, that they make it easier to visualize the phenomena and recognize cause and effect, make the postulates of Bryant's theory unnecessary, lead to simpler and faster calculations, and make the theory applicable to more general starting conditions. This will be demonstrated with examples of simple systems with up to four dissolved species and two precipitates. The extension to systems with additional, nonprepitating species will be described.

Systems and Premises

The systems to be considered are of the following type. A fluid containing ions flows through an inert, permeable medium; precipitates are deposited wherever the solubility product of the respective solid becomes exceeded, and are dissolved wherever the fluid becomes unsaturated with respect to them.

Since the purpose of this presentation is to demonstrate the applicability of concepts and tools, not to propose an elaborate theory, stringent premises are introduced for the sake of simplicity and clarity. These premises are:

- The fluid and the permeable medium are incompressible
- The system is isothermal
- The flow is unidimensional
- The flow is ideal, that is, no hydrodynamic dispersion
- The flow rate is constant
- The fractional pore volume of the medium is uniform and constant
- The fluid and any precipitates are in local equilibrium
- The precipitates remain stationary
- The precipitates occupy a negligible fraction of the pore volume
- The solubility-product relations are obeyed in terms of concentrations (i.e., activity coefficient effects are disregarded)

These premises are essentially the same as in Bryant's simplified theory. Systems to be considered involve univalent ions $A, B, \ldots$ of one charge sign; $X, \ldots$ of opposite charge sign; neutral molecules M; and precipitates AX and BX. All ions are assumed to be univalent. Situations to be discussed are Riemann problems and a simple case showing the fate of a precipitate bank being leached by an unsaturated fluid.

Most of the premises, except for those of incompressibility, isothermal behavior, and unidimensional flow, can be relaxed at little cost in mathematical complexity, as demonstrated in multicomponent chromatography theory (Helfferich and Klein, 1970, Ch. 5) and noted by Bryant. They are used here to keep the presentation of principles as simple as possible.

Concepts, Basic Equations, and Tools of Chromatographic Theory

For ease of later reference a brief review of the fundamental concepts of theory of multicomponent chromatography (Helfferich and Klein, 1970) is in order.

The two most important concepts are those of waves and coherence.

A wave is any variation of dependent variables, in the case at hand of fluid- or solid-phase concentrations (waves were called boundaries, fronts, transitions, or mass-transfer zones in the earlier literature). A wave may be self-sharpening, nonsharpening, or indifferent. A self-sharpening wave becomes or remains a shock. In the absence of dissipation a shock is a discontinuity; in real systems, dissipation (characterized by a finite Peclet number) lets the shock attain a constant pattern, that is, an abrupt but continuous variation that travels without further sharpening or spreading. A nonsharpening wave spreads regardless of dissipation and initial condition, and retains or approaches a proportionate pattern in which its diffuseness increases in proportion to the distance traveled. An indifferent wave in the absence of dissipation travels without change in sharpness; in real systems, dissipation makes it spread in proportion to the square root of distance traveled.

The fundamental equation of chromatography is the wave equation, giving the velocity at which a given concentration C_i of a species travels in the direction of fluid flow (Helfferich and Klein, 1970, pp. 41–45):

$$u_{C_i} = (\partial z/\partial t)_{C_i} = u^o(\partial C_i/\partial \tilde{C}_i)_z \tag{1}$$

where $\tilde{C}_i$ is the overall concentration of i, that is, the total amount per unit pore volume, and u^o is the velocity of fluid flow. Equation 1 is readily obtained from a material balance for species i in a differential layer normal to the direction of flow

$$(\partial \tilde{C}_i/\partial t)_z = -u^o(\partial C_i/\partial z)_t \tag{2}$$

with the chain rule for interdependence of partial derivatives. No assumptions are involved other than unidimensional flow in the z direction and transport in flow direction exclusively by convection ($J_i = u^o C_i$). In particular, no continuous and differentiable relation between $\tilde{C}_i$ and C_i is required.

The wave equation, Eq. 1, does not apply to discontinuities—for example, to shocks in the absence of dissipation—because for these a specific concentration cannot be defined. Instead, the shock velocity $u_{\Delta C_i}$ is given by

$$u_{\Delta C_i} = u^o(\Delta C_i/\Delta \tilde{C}_i) \tag{3}$$

where Δ indicates the difference across the discontinuity (downstream value minus upstream value). This equation is obtained from an integral material balance over the discontinuity instead of the differential balance, Eq. 2.

The key concept is that of coherence. As a chromatographic column responds to an input variation, a pattern is generated or approached in which all waves obey the coherence condition of equal wave (or shock) velocities of all components present; at any point in space and time:

$$u_{C_i} = \lambda \quad \text{differential coherence condition} \tag{4}$$

or

$$u_{\Delta \tilde{C}_i} = \Lambda \quad \text{integral coherence condition} \tag{5}$$

where λ or Λ has the same value for all species. In the language of mathematics of waves (Rhee and Amundson, 1970; Aris and Amundson, 1973; Jeffrey, 1976), all waves in a coherent pattern are simple waves. In a Riemann problem without dissipation, coherence is immediately attained and then maintained throughout. For a proof of attainment of, or development toward, coherence from arbitrary starting conditions, see Helfferich (1986).

An important tool of coherence theory is the composition path diagram. Composition paths are defined as curves in the composition space (with species concentrations as coordinates) along which the differential coherence condition is obeyed. (In the more refined language of mathematics, the composition paths are generalized Γ characteristics in the hodograph space; see Rhee et al., 1970.) The grid of paths is given by the fundamental equilibrium and flow equations of the systems and the values of the parameters in these equations, but is independent of the initial and feed conditions. Since the response develops into a coherent pattern, the eventual state of the system traces a route that runs exclusively along such paths (with qualifications for

shocks, as will become apparent later). The grid of paths thus can serve as a road map: once established, it can be used to predict the response of a given system under any operating conditions. By convention, composition routes of waves are shown as arrows pointing in the direction of flow, that is, from the composition on the upstream side of the wave to that on the downstream side.

The basic material balance, Eq. 2, is valid for precipitation/dissolution systems as well. In principle, therefore, the concepts and tools developed for multicomponent chromatography can be applied here, too. In fact, the construction of composition paths turns out to be much simpler than in chromatography. While it is true that the mentioned proof of attainment of coherence is restricted to hyperbolic equations and does not cover the situations encountered here, the validity of the concept has been borne out by all of the great number of numerical calculations performed by Walsh et al. (1984), Bryant et al. (1986, 1987), and Dria et al. (1987).

Systems A, B, X, AX and A, B, X, AX, BX

Composition space and phase diagrams

For construction of composition paths and routes, the concentrations to be used as coordinates for the composition space must be decided on. The conventional choice in chromatography is that of the fluid-phase concentrations, C_i. In principle, solid-phase or overall concentrations, $\bar{C}_i$ or $\tilde{C}_i$, respectively, could be used instead, but they are inconvenient because they cannot directly describe effluent concentrations. For precipitation/dissolution systems, in contrast, the best choice is that of the overall concentrations, $\tilde{C}_i \equiv C_i + \bar{C}_i$ (note that all concentrations are per unit volume of fluid.) This is so because the system will develop waves across which the fluid-phase concentrations change while the solid-phase concentrations remain constant, or the converse, whereas the overall concentrations will always vary if one or both of the other sets do. In addition and for the same reason, the overall concentrations are the coordinates of choice for phase diagrams, which greatly help one to understand the physics of the systems.

The phase diagrams of the systems A, B, X, AX and A, B, X, AX, BX are shown in Figures 1 and 2. Of course, all regions contain fluid, exclusively or in addition to the precipitates listed.

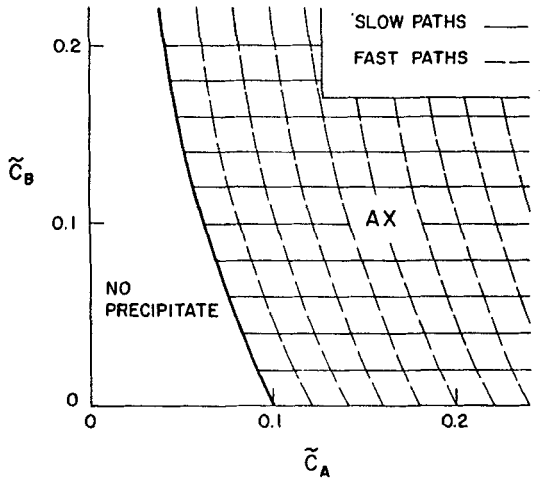

Figure 1. Phase diagram and composition paths, system *A, B, X, AX*.
$K_{AX} = 0.01$

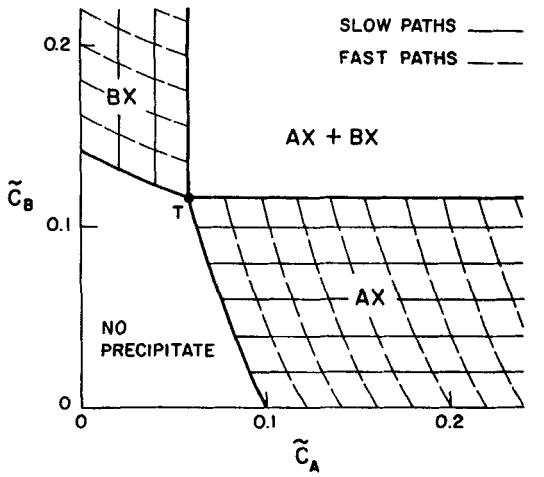

Figure 2. Phase diagram and composition paths, system *A, B, X, AX, BX*.
$K_{AX} = 0.01$; $K_{BX} = 0.02$; T = triple point

The diagram of the system A, B, X, AX, Figure 1, is constructed as follows. The relevant conditions are

$$C_A + C_B = C_X \quad \text{charge balance} \tag{6}$$

$$C_A C_X \leq K_{AX} \quad \text{solubility product} \tag{7}$$

In the AX region (i.e., with AX present) and at its border, the equality sign in condition (Eq. 7) applies. Thus, here, after elimination of C_X between Eqs. 6 and 7:

$$C_B = K_{AX}/C_A - C_A \tag{8}$$

This is the equation for the border (note that at the border, as within the no-precipitate region, $\bar{C}_i = 0$, so that $\tilde{C}_i = C_i$).

The diagram of the system A, B, X, AX, BX, Figure 2, is constructed as follows. Conditions Eqs. 6 and 7 apply, and in addition,

$$C_B C_X \leq K_{BX} \tag{9}$$

The border of the BX regions is described by Eq. 8 with A and B interchanged. The borders of the AX and BX regions are plotted as above up to their intersection. This is the triple point, T, at which the solution is saturated with respect to both AX and BX. In the $AX + BX$ region, at its borders, and at T, Eqs. 6, 7, and 9 uniquely fix the three fluid-phase concentrations C_A, C_B, and C_X:

$$C_A = K_{AX}/(K_{AX} + K_{BX})^{1/2} \tag{10}$$

$$C_B = K_{BX}/(K_{AX} + K_{BX})^{1/2} \tag{11}$$

$$C_X = (K_{AX} + K_{BX})^{1/2} \tag{12}$$

Thus, in the $AX + BX$ region the fluid composition is invariant and, in that region,

$$\tilde{C}_i = \bar{C}_i + C_i^T \tag{13}$$

In other words, both AX and BX are present where, and only where, the overall concentrations of both A and B exceed the respective triple-point concentrations, given by Eqs. 10 and 11.

Composition path diagrams

By definition, the paths are curves along which the differential coherence condition, Eq. 4, is met, that is, for which at any point the wave velocities, Eq. 1, of all species present are equal. The composition space is completely covered by an infinite number of paths, of which only some at regular intervals are shown on diagrams.

Also, in a coherent wave, fluid-phase, solid-phase, and overall concentration velocities are automatically equal as all concentrations coexisting at one point travel jointly and so remain in one another's company. Equations 1 and 3 thus also give the respective velocities of overall concentrations and steps.

In the absence of any precipitate, $d\bar{C}_i = 0$ and thus $d\tilde{C}_i = dC_i$ for all species. With the wave equation, Eq. 1, this gives

$$u_{C_i} = u^o \quad \text{for all } i \tag{14}$$

Accordingly, regardless of its direction in the composition space, any composition variation within the no-precipitate region is coherent and travels at the velocity u^o of fluid flow: The region is pathless.

In the $AX + BX$ region of the system A, B, X, AX, BX the fluid-phase composition is invariant, that is, $dC_i = 0$ for all i. With wave Eq. 1 (applied to the overall concentration velocity) this gives

$$u_{\tilde{C}_i} = 0 \quad \text{for all } i \tag{15}$$

In other words, any composition variation in such a region is coherent and is a standing wave. This region thus is also pathless.

In the AX region in the systems A, B, X, AX and A, B, X, AX, BX, the coherence condition, Eq. 4, requires that $u_{\tilde{C}_A} = u_{\tilde{C}_B}$. However, for any nonprecipitating ion, such as B in this case, the overall concentration necessarily equals the fluid-phase concentration, and thus the wave velocity of such an ion according to wave Eq. 1 is equal to u^o. That is:

- Any concentration variation of a nonprecipitating species is propagated at the velocity of fluid-phase flow.

For ion A in the AX region, the coherence condition, Eq. 4, then requires that $u_{\tilde{C}_A} = u^o$. The wave equation shows that this calls for $d\tilde{C}_A = dC_A$, which amounts to $d\bar{C}_A = 0$. Accordingly, curves with constant precipitate concentration $\bar{C}_A$ are paths with fluid velocity. These "fast" paths, shown in Figures 1 and 2 as dashed curves, are parallel to the border of the AX region with the no-precipitate region. The BX region contains analogous paths.

The only instance in which the requirement $u_{\tilde{C}_k} = u^o$ for a nonprecipitating species k lapses is along lines $d\tilde{C}_k = 0$. For these, $dC_k = 0$ also (since $\bar{C}_k = 0$), so that the wave velocity u_{C_k} becomes indefinite. In the AX region, $\tilde{C}_A$ and $\tilde{C}_X$ vary by equal amounts along such lines, that is, AX is precipitated or dissolved without change in fluid-phase composition. With $dC_A = 0$ for such lines, the wave equation then gives $u_{\tilde{C}_A} = 0$. In other words, the lines of constant $\tilde{C}_A$ in the AX region (parallel to the A axis) are loci of invariant fluid-phase composition and correspond to coherent standing waves. The BX region contains analogous paths. These "slow" paths are shown in Figures 1 and 2 as thin solid lines.

Composition routes and profiles

Multicomponent chromatography theory has shown that, in the absence of dissipation, the response to a Riemann problem is coherent from the outset (Helfferich and Klein, 1970; Helfferich, 1986). In addition, a faster wave in such a pattern must be downstream of a slower one, both having originated at the same place and time. The construction of a composition route describing the events developing from an initial, discontinuous variation between uniform upstream and downstream compositions thus calls for finding a way in the composition diagram from the upstream to the downstream point, subject to the coherence condition and with waves in the proper sequence of velocities. The only complication is that the response may involve shocks. The composition points upstream and downstream of such a shock must meet the integral coherence condition, Eq. 5, but are not necessarily on the same path, the paths having been obtained from the differential coherence condition, Eq. 14.

Once the composition route has been found, concentration profiles or histories are easily constructed with use of the wave velocities obtained from Eq. 3.

System A, B, X, AX

In principle, four situations can arise as the upstream and downstream composition points, U and D, may be:

1. Both in the no-precipitate region
2. Both in the AX region
3, 4. In different regions with AX upstream or downstream, respectively

The four cases are illustrated in Figures 3 to 5. In all examples the path grid is the same as in Figure 1 (same value of K_{AX}).

In case 1, shown in Figure 3, the route leads directly from U to D, reflecting a wave of fluid velocity. Inasmuch as the wave velocity remains constant along the entire route, the wave is indifferent with respect to sharpening properties; that is, it remains discontinuous in the absence or dissipation, but in real

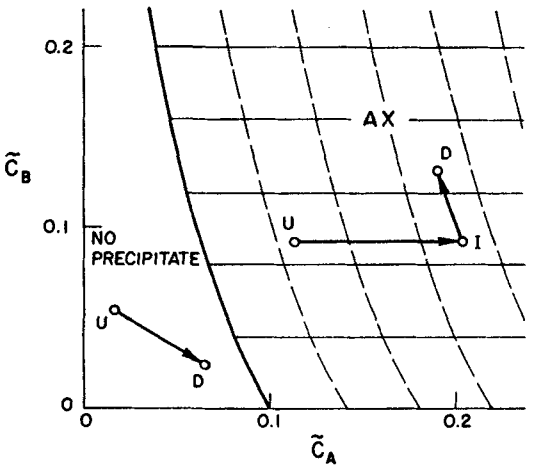

Figure 3. Composition routes, system *A, B, X, AX*.
Cases 1, 2: precipitate on both sides or neither side of starting variation
$K_{AX} = 0.01$

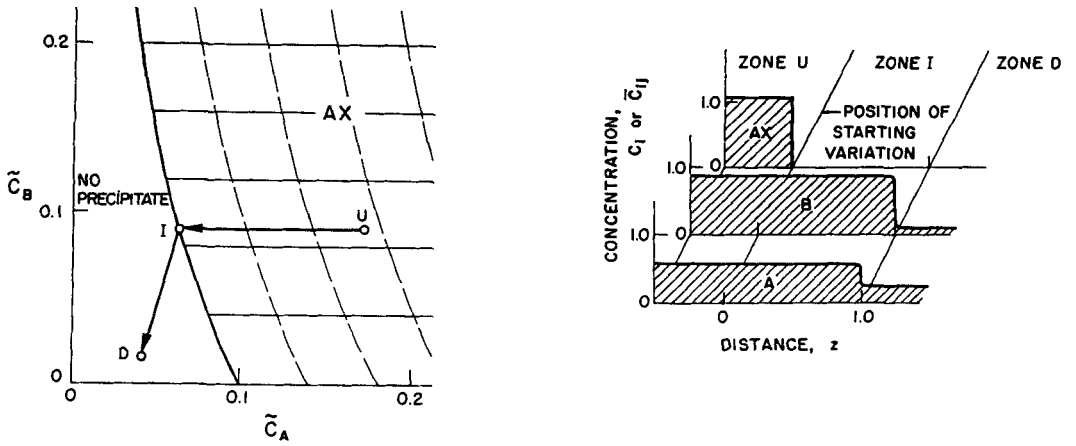

Figure 4. Composition route and profiles, system *A*, *B*, *X*, *AX*.
Case 3: precipitate upstream but not downstream of starting variation
$K_{AX} = 0.01$; $u^o = 1.0$; starting variation at $z = 0$; profiles at $t = 1.0$

systems with dissipation spreads in proportion to the square root of traveled distance. Thus, in a real system the compositions along the straight-line route will become realized as linear combinations of U and D are generated. Should the straight line UD intersect the envelope of the AX region, the route will be squeezed out of that region because within the latter it cannot find paths in the required sequence.

In case 2, Figure 3, the route follows the slow path (zero velocity) from U, then switches to the fast path (velocity u^o) leading to D. The slow wave is a standing wave along which only the amount of precipitate changes. Since the (stationary) precipitate is not subject to dissipation, this wave retains its initial sharpness. The fast wave travels at fluid velocity and involves no change of precipitate concentration. It is an indifferent wave and spreads accordingly under the effect of dissipation. Between the two waves, a zone of composition I forms and grows in length in proportion to elapsed time.

In case 3, shown in Figure 4, the route follows the slow path from U to the border of the AX region and then leads directly to D across the pathless region. The slow wave again is a standing wave with the same properties as that in case 2, and the fast wave has the same properties as that in case 1. The intermediate zone I contains no precipitate AX but is saturated with respect to it.

In case 4, Figure 5, no permissible route based on the differential coherence condition can be found because a fast variation outside the AX region is necessarily upstream of a slower one within that region. Under such conditions a shock develops. The shock must meet the integral coherence condition, Eq. 5, but the pair of points U and D in general does not. This is because any concentration variation of the nonprecipitating ion B, whether a shock or not, necessarily travels at the fliud velocity whereas the concentration variation of A is necessarily retarded by a change in precipitate concentration. It follows that the shock can only be coherent if it involves no concentration variation of B:

- A composition route may enter the region of a precipitate from that of no precipitate only along a locus of constant concentrations of nonprecipitating ions.

The corresponding wave is a shock with velocity less than that of the fluid. In the case at hand,

$$u_\Delta = u^o(\Delta C_A/\Delta \tilde{C}_A) = u^o(C_A^a - C_A^U)/(\tilde{C}_A^I - C_A^U) \quad (16)$$

where superscript I refers to the downstream point of the shock,

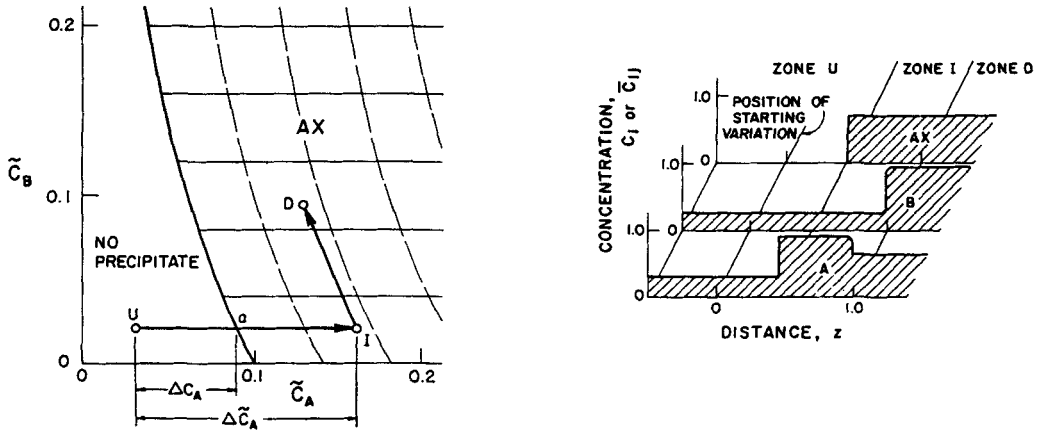

Figure 5. Composition route and profiles, system *A*, *B*, *X*, *AX*.
Case 4: precipitate downstream but not upstream of starting variation
$K_{AX} = 0.01$; $u^o = 1.0$; starting variation at $z = 0$; profiles at $t = 1.0$
Variations in C_A and $\tilde{C}_A$ across shock UI are indicated

and superscript a to the intersection with the border of AX, Figure 5 (note that $C_A^I = C_A^a$ since the slow paths, which include aI, are curves of constant C_A). This slow shock UI is followed by a fast, indifferent wave ID of fluid velocity and involving no variation of precipitate concentration.

For algebraic calculation of the velocity of the shock UI from Eq. 16 and input data, the values of $\tilde{C}_A^I$ and C_A^a must first be determined. Noting that $\overline{C}_A^I = \overline{C}_A^D$ because of the constant precipitate concentration along ID, one has

$$\tilde{C}_A^I = \overline{C}_A^D + C_A^a \tag{17}$$

At a, Eqs. 6 and 7 apply and can be solved for C_A, noting that $C_B^a = C_B^U$:

$$C_A^a = \frac{1}{2}\{[(C_B^U)^2 + 4K_{AX}]^{1/2} - C_B^U\} \tag{18}$$

All these results for the system A, B, X, AX can be arrived at by simple reasoning without chromatographic theory. Case 1 is a classical fluid-phase concentration wave in a system with convection and no solid phase. The only new result here is the deformation of the route under the effect of dissipation if the straight line UD cuts through the AX region. Case 2 shows that a fluid-phase composition variation over a solid, in the absence of precipitation or dissolution, travels at fluid velocity—a trivial result as the solid does not participate and could as well be removed. It also shows that a saturated fluid flowing over a precipitate does not alter the latter's concentration, even if that concentration is not uniform, an equally obvious result. Case 3 shows what happens at the downstream end of a bank of precipitate with saturated fluid of uniform concentration: There is neither dissolution nor additional precipitation, and saturated fluid emerging from the bank displaces the original, unsaturated fluid at fluid velocity, Figure 4. The physics of the system make it self-evident that this must be so. Case 4 shows what happens at the upstream end of a bank of precipitate with saturated fluid at uniform concentration when an unsaturated fluid enters from upstream: Precipitate is dissolved, letting the upstream boundary of the bank recede at a velocity less than that of the fluid; at the same time, the saturated fluid generated by this dissolution displaces the original saturated fluid over the precipitate at fluid velocity and without dissolution or precipitation, Figure 5. This result, too, is apparent from physics alone. The examples of the A, B, X, AX system thus only serves to illustrate theory and technique and to validate these by comparison with known behavior.

System A, B, X, AX, BX

Here, the upstream and downstream composition points of the initial discontinuity can each be in one of four regions: no precipitate, AX, BX, or $AX + BX$. This makes for a total of sixteen possible combinations, listed in Table 1. Only some of these, however, are of real interest; they are illustrated in Figures 6 to 12. In all examples the path grid is the same as in Figure 2 (same values of K_{AX} and K_{BX}). The shock velocities, required for profile construction, are obtained from Eq. 3 by a procedure as in case 4 of the previous system (Figure 5 or Eqs. 16–18), noting that $C_A = C_A^a$ in the AX region along the path through a, $C_B = C_B^b$ in the BX region along the path through b, and $C_i = C_i^T$ $(i = A, B)$ everywhere in the $AX + BX$ region.

Cases 1, 2, 3, 5, and 6 have strict and obvious analogues in cases 1, 2, and 3 of the previous system. Case 4, with both U and D in the $AX + BX$ region, is trivial as any variation within that region is a standing wave with change only in precipitate concentrations.

Table 1. Possible Distributions of Upstream and Downstream Starting Compositions over Regions in Phase Diagram

Case	Region			
	No Precip.	AX	BX	$AX + BX$
1	U, D			
2		U, D		
3			U, D	
4				U, D
5	D	U		
6	D		U	
7	D			U
8	U	D		
9	U		D	
10	U			D
11		D		U
12			D	U
13		U		D
14			U	D
15		U	D	
16		D	U	

Case 7, with U in the $AX + BX$ region and D in the no-precipitate region, is illustrated in Figure 6. The route leads from U directly to the triple point, and then directly to D. The first wave, UT, is a standing wave involving a variation only of the precipitate concentrations; the second wave, TD, is an indifferent wave of fluid velocity in the absence of precipitate. In terms of physical behavior, the downstream end of a bank of precipitate and saturated fluid remains unchanged. From the bank, fluid of triple-point composition, T, emerges and displaces the original, unsaturated fluid at fluid velocity.

Case 8, with U in the no-precipitate region and D in the AX region, is illustrated in Figure 7. As long as the upstream concentration of B is below the triple-point value, that is, $C_B^U < C_B^T$,

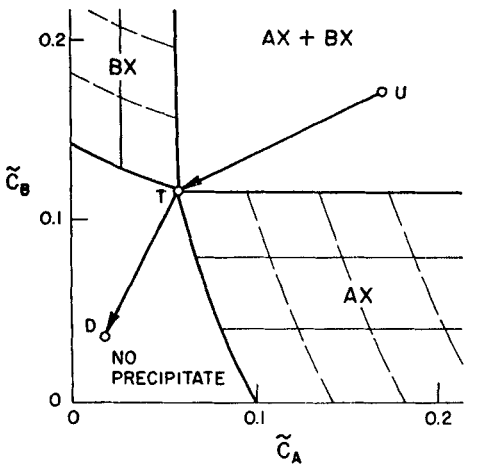

Figure 6. Composition route, system *A, B, X, AX, BX*.
Case 7: precipitates AX, BX upstream but not downstream of starting variation
$K_{AX} = 0.01$; $K_{BX} = 0.02$; $u^o = 1.0$

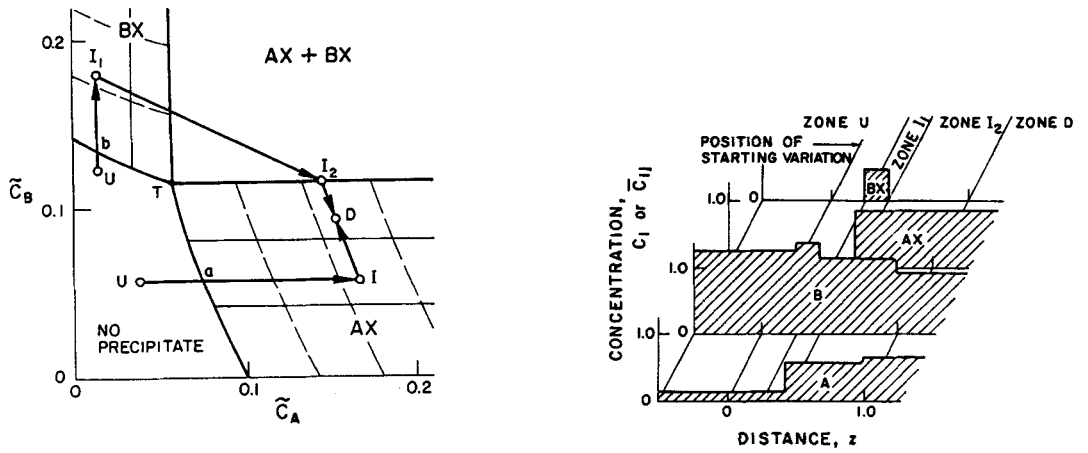

Figure 7. Composition routes and profiles, system *A*, *B*, *X*, *AX*, *BX*.
Case 8: *AX* downstream but not upstream of starting variation
$K_{AX} = 0.01$; $K_{BX} = 0.02$; $u^o = 1.0$; different compositions of upstream fluid
Starting variation at $z = 0$; profiles at $t = 1.0$ and for route through *BX* region

the behavior is the same as in case 4 of the previous system. However, if C_B^U exceeds C_B^T, the route no longer has a permissible direct entry into the *AX* region. The only way to enter any precipitate region is along UI_1 (line of constant $\tilde{C}_A$) into the *BX* region. This wave is a slow shock. Because of the absence of paths leading from the *BX* to the *AX* region, the next wave must also be a shock. The route of this shock is easier to find if the behavior at point *D* is considered first. The last part of the route should be the fastest, and so will correspond to I_2D, an indifferent wave of fluid velocity with a route along the fast path through *D*. The location of point I_1, which must meet the integral coherence condition with I_2, can now be found as follows. The coherence condition, Eq. 5, requires that

$$(C_A^{I2} - C_A^{I1})/(\tilde{C}_A^{I2} - \tilde{C}_A^{I1}) = (C_B^{I2} - C_B^{I1})/(\tilde{C}_B^{I2} - \tilde{C}_B^{I1}) \quad (19)$$

but $C_A^{I1} = C_A^b$, $C_A^{I2} = C_A^T$, $C_B^{I1} = C_B^b$, and $C_B^{I2} = C_B^T$, Figure 7, so that

$$(C_B^{I2} - C_B^{I1})/(\tilde{C}_A^{I2} - \tilde{C}_A^{I1}) = (C_B^T - C_B^b)/(C_A^T - C_A^b) \quad (20)$$

In other words, the line I_1I_2 must have the same slope as, and so be parallel to, the line bT, where T is the triple point and b is the intersection of the line UI_1 with the border of the *BX* region. Thus, knowing I_2 as the end point of the fast path through *D*, one can find I_1 as the intersection of the parallel to bT through I_2 with the line of constant $\tilde{C}_A = C_A^U$, Figure 7. Alternatively, $\tilde{C}_B^{I1}$ can be calculated algebraically from Eq. 20 after replacements $\tilde{C}_A^{I2} = \bar{C}_A^D + C_A^T$, $\tilde{C}_A^{I1} = C_A^b = C_A^U$, and $\tilde{C}_B^{I2} = C_B^T$:

$$\tilde{C}_B^{I1} = C_B^T + (\bar{C}_A^D + C_A^T - C_A^U)(C_B^T - C_B^b)/(C_A^T - C_A^U) \quad (21)$$

Here, the triple point concentrations C_i^T are given by Eqs. 10 and 11, and C_B^b is given by Eq. 18 with *A* and *B* interchanged. Once $\tilde{C}_B^{I1}$ and C_B^b are known, the velocity of the slow shock, UI_1, is easily calculated from Eq. 3:

$$u_{\Delta(UI_1)} = u^o \Delta C_B/\Delta\tilde{C}_B = u^o(C_B^b - C_B^U)/(\tilde{C}_B^{I1} - C_B^U) \quad (22)$$

The complete route is UI_1I_2D, with a slow shock UI_1, a faster shock I_1I_2 (it is easily shown that this shock is faster if $C_B^U > C_B^T$), and a still faster, indifferent wave I_2D of fluid velocity. The profile shown in Figure 7 is for this case.

Physically, the route UI_1I_2D corresponds to the following situation at the upstream end of a bank of precipitate *AX* (point *D*) receiving a fluid unsaturated with respect to *AX* and *BX* and rich in *B* (point *U*). The rear boundary of *AX* recedes, remaining sharp (shock I_1I_2); where *AX* dissolves, *BX* is precipitated; the rear boundary of the bank of *BX* so formed (point I_1) recedes remaining sharp, but more slowly (shock UI_1), as *BX* is dissolved again by arriving fresh, unsaturated fluid (*U*); meanwhile, fluid saturated with respect to both *AX* and *BX* (I_2) displaces the original fluid in the *AX* bank (*D*) at fluid velocity (wave I_2D).

Unfortunately, the solution UI_1I_2D shown in Figure 7 and discussed above is not unique. An alternative solution obeying all equations and conditions is shown in Figure 8. Instead of three distinct waves UI_1, I_1I_2, and I_2D it contains only two, *UI* and *ID*. The latter is a step and, as is easily shown, meets the coherence condition if the line *ID* is parallel to *ba* (*b* and *a* being the inter-

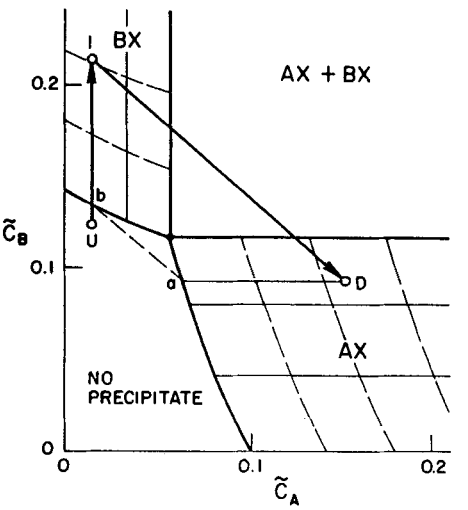

Figure 8. Alternative unstable composition route for system in Figure 7 with high concentration of *B* in fluid upstream of starting variation.

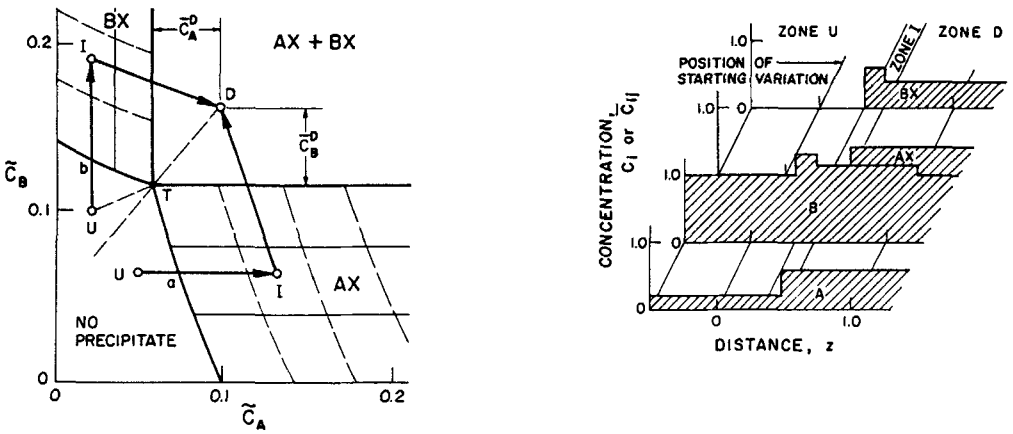

Figure 9. Composition routes and profiles, system *A*, *B*, *X*, *AX*, *BX*.
Case 10: *AX*, *BX* downstream but not upstream of starting variation
$K_{AX} = 0.01$; $K_{BX} = 0.02$; $u^o = 1.0$; different compositions of upstream fluid
Starting variation at $z = 0$; profiles at $t = 1.0$ and for route through *BX* region

sections of *UI* and of the slow path through *D* with the borders of *BX* and *AX*, respectively). However, this solution is unstable: Dissipation in a real system causes intermediate compositions along the route to be realized. Compositions in the *AX* region are downstream of those in the *AX* + *BX* region and run away from them as they move essentially at fluid velocity while those in *AX* + *BX* are stationary. Also, within the *BX* and *AX* regions, the straight-line route *ID* is noncoherent; development toward coherence (slow paths upstream of fast paths) distorts the route downward in *BX* and upward in *AX*. The overall effect is that the system will approach the stable route UI_1I_2D of Figure 7. Moreover, the route *ID* corresponds to a step but not a shock as it does not meet the requirement that, in the solution to the differential equations, the upstream composition would overtake all others.

In more general and loose terms: A step, even if meeting the integral coherence condition, is usually not stable if its straight-line route traverses a region or regions of low or zero wave velocity between others of higher wave velocity, or vice versa.

Case 9 is the exact mirror image of case 8, with *A* and *B* interchanged.

Case 10, with *U* in the no-precipitate region and *D* in the *AX* + *BX* region, is illustrated in Figure 9. As long as point *U* is below the extension of the line *DT*, the route enters *AX* as in previous cases and then turns to *D* at point *I*. The segment *UI*, parallel to the *A* axis, is a slow shock. Point *I* is found in a manner analogous to the construction in case 8, Figure 7, as the intersection of the parallel to *Ta* through *D* with the line of constant $\tilde{C}_A = C_A^U$. The segment *ID*, with *D* in a region of zero wave velocity, is another, faster shock. The velocity of the shock *UI* can be calculated with Eqs. 16 to 18; that of the shock *DU*, with Eq. 22.

If point *U* is moved closer to the extension of *DT*, the velocities of the two shocks become more similar. With *U* on that extension, they are equal as the ratios *Ua*:*UI* (proportional to the velocity of *UI*) and *UT*:*UD* (proportional to the velocity of *ID*) become equal, and the two shocks merge into a single one, *UD*. With *U* above the extension of *DT*, the requirement that the faster shock must be upstream of the slower one forces the route to enter the *BX* instead of the *AX* region on its way to the *AX* + *BX* region. The profiles shown in Figure 9 are for this case.

In terms of physics, when a bank of mixed precipitate *AX* + *BX* receives an unsaturated fluid, both precipitates dissolve, but in general one of them recedes faster than the other. Which one this is depends on the relative solubilities, relative amounts of precipitates, and relative concentrations of precipitating ions in the arriving fluid. An algebraic criterion is:

$$\text{Route through } AX \text{ if } \frac{\bar{C}_A^D(C_B^T - C_B^U)}{\bar{C}_B^D(C_A^T - C_A^U)} < 1$$

$$\text{Route through } BX \text{ if } \frac{\bar{C}_A^D(C_B^T - C_B^U)}{\bar{C}_B^D(C_A^T - C_A^U)} < 1 \qquad (23)$$

with the C_i^T given by Eqs. 10 and 11. This criterion is easily derived as follows. The route was shown to lead through the *AX* region if point *U* is below the extension of *DT*, that is, if the slope of *UT* is greater than that of *TD*, Figure 9. If so, then

$$(C_B^T - C_B^U)/(C_A^T - C_A^U) > \bar{C}_B^D/\bar{C}_A^D \qquad (24)$$

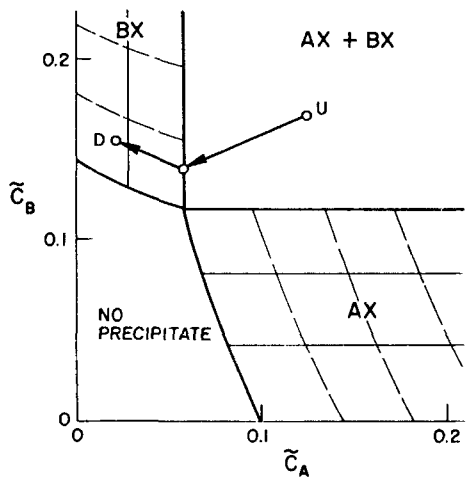

Figure 10. Composition route, system *A*, *B*, *X*, *AX*, *BX*.
Case 12: *AX* and *BX* upstream, *BX* downstream of starting variation
$K_{AX} = 0.01$; $K_{BX} = 0.02$; $u^o = 1.0$

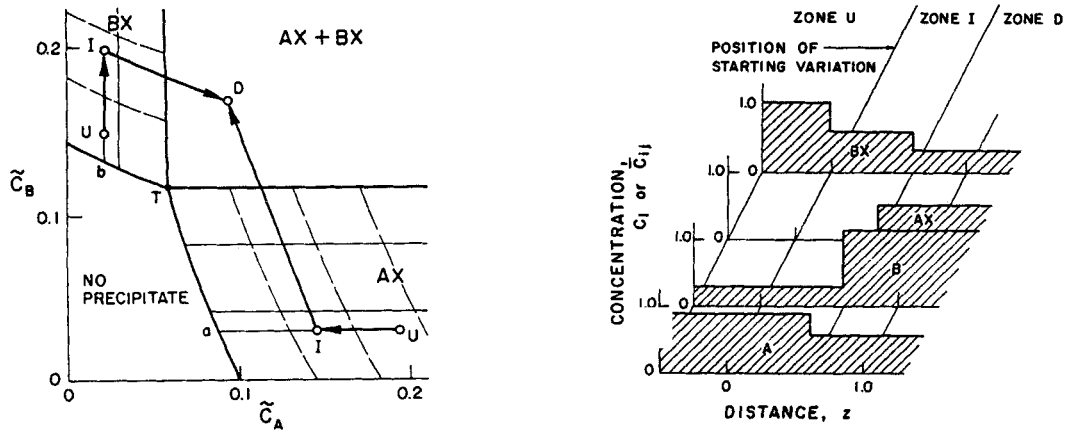

Figure 11. Composition routes and profiles, system *A, B, X, AX, BX.*

Case 13: *AX* and *BX* downstream, *AX* upstream of starting variation
$K_{AX} = 0.01$; $K_{BX} = 0.02$; $u^o = 1.0$
Starting variation at $z = 0$; profiles at $t = 1.0$

Obviously, for a route through the *BX* region the inequality is reversed. The criterion of Eq. 23 follows directly from this.

For cases 11 and 12, with *U* in the *AX* + *BX* region and *D* in the *AX* or *BX* region, the construction is straightforward and the conclusions are trivial. In case 12 (*BX* downstream, Figure 10) the pattern consists of a standing wave *UI* and an indifferent wave *ID* at fluid velocity. All that happens physically is that downstream of the bank of *AX* + *BX*, the fluid over *AX*, which at the start is unsaturated with respect to *BX*, is displaced at fluid velocity by one that is saturated with respect to both precipitates.

Cases 13 and 14, with *U* in the *AX* or *BX* region and *D* in the *AX* + *BX* region, are also simple. In case 13, Figure 11, with (*AX* upstream), the entry from the *AX* into the *AX* + *BX* region, where the wave velocities are zero, can only be by way of a coherent shock. This shock *ID* will be downstream of a standing wave *UI* with route parallel to the *A* axis. For the shock to be coherent, the line *DI* must be parallel to *Ta*, as an argument analogous to that in case 8 shows. Physically, what happens is that the rear boundary of the bank of mixed precipitate recedes, *BX* being dissolved by *BX*-unsaturated fluid from the *AX* bank upstream. A concentration variation of precipitate *AX* remains stationary at the location of the initial border between pure and mixed precipitates. Fluid-phase concentrations do not vary across this step. The velocity of the shock *ID* can be calculated as in the previous cases involving shocks between the *AX* (or *BX*) and *AX* + *BX* regions.

Cases 15 and 16, with *U* and *D* in different regions *AX* and *BX*, are very similar to the variants of cases 7 and 8 involving both precipitates, and the construction establishing the intermediate wave is analogous. In case 16 (*BX* upstream, Figure 12) there is a standing wave UI_1 across which only the concentration of precipitate changes, a shock I_1I_2 at less than fluid velocity and with route parallel to the line *bT*, and an indifferent wave I_2D at fluid velocity and involving only fluid-phase concentration variations. In terms of physics, the border between precipitates *BX* and *AX* (wave I_1I_2) moves downstream as a shock; at this shock, *AX* is dissolved by unsaturated fluid from *BX*, while *X* so liberated precipitates *BX*. In the absence of dissipation there is no overlap of *AX* and *BX*; with dissipation the route will be somewhat deformed downward and the precipitates may be expected to overlap slightly within the shock. Upstream of the *BX*/*AX*

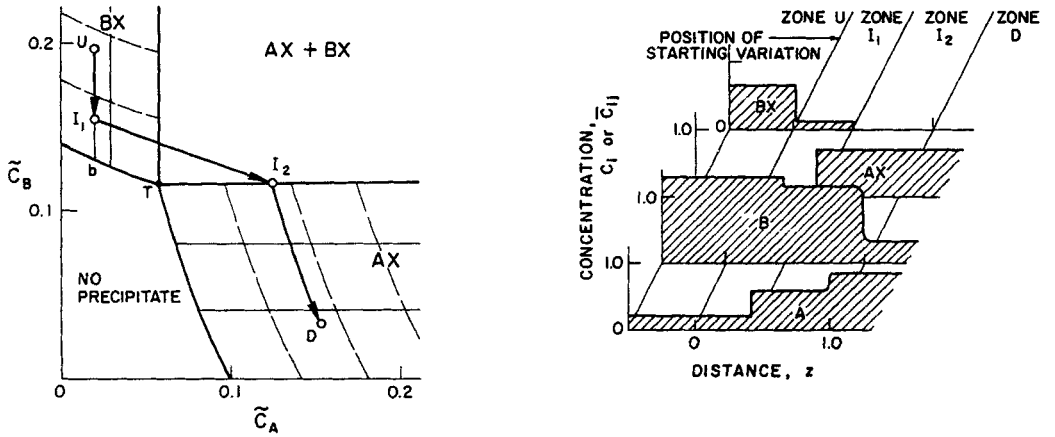

Figure 12. Composition route and profiles, system *A, B, X, AX, BX*

Case 16: *BX* upstream, *AX* downstream of starting variation
$K_{AX} = 0.01$; $K_{BX} = 0.02$; $u^o = 1.0$
Starting variation at $z = 0$; profiles at $t = 1.0$

shock there is and remains a discontinuous concentration variation of BX (standing wave UI_1) at the location of the original BX/AX boundary; fluid-phase concentrations do not vary across this step. Downstream of that location, fluid saturated with respect to both AX and BX (triple-point composition) displaces the original, BX-unsaturated fluid over AX in an indifferent wave at fluid velocity and without variation in precipitate concentration (wave I_2D). The shock velocity can be calculated as in previous analogous cases.

Sample Problem

The application of the concept will be illustrated with a simple example from the system A, B, X, AX, BX. Assume a bank of precipitate AX and fluid containing both A and B (point P) is positioned between unsaturated fluid rich in B upstream (point U) and fluid lean in both A and B downstream (point D).

Figure 13 shows the composition routes; Figure 14, the distance-time diagram; Figure 15, transient composition profiles. As flow is started, the pattern developing from the upstream end of the bank is UI_1I_2P and that from the downstream end is PaD, corresponding to cases 8 (Figure 11) and 4 (Figure 8), respectively, discussed above; the overall route thus is UI_1I_2PaD. The distance-time diagram shows shocks UI_1 and I_1I_2, an indifferent wave I_2P of fluid velocity, a standing wave Pa, and an indifferent wave aD of fluid velocity. AX is dissolved at the upstream end of the bank but is not precipitated downstream. BX is precipitated upstream of the shrinking AX bank but is redissolved, so that in effect a growing zone of BX migrates downstream. Over the AX bank, fluid saturated with respect to $BX(I_2)$ displaces the original fluid (P) at fluid velocity. Fluid saturated with respect to AX but not BX, a, exists from the AX bank and displaces the original fluid downstream (D) at fluid velocity. All fluid-velocity waves are indifferent.

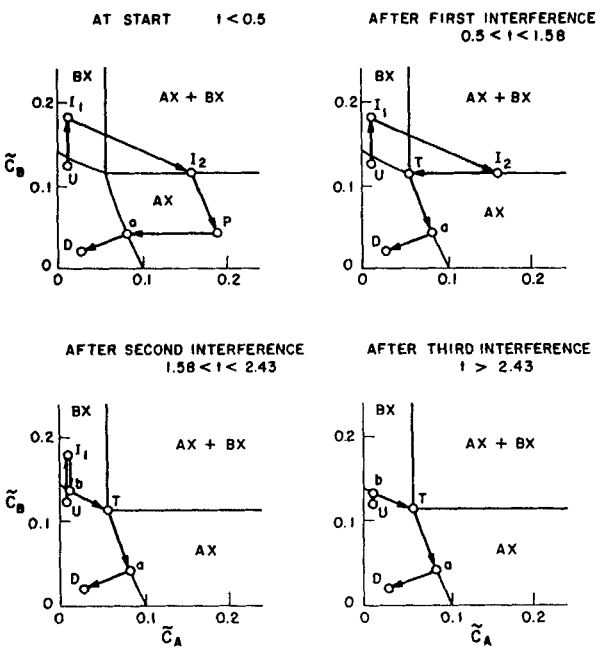

Figure 13. Transient composition routes for sample case, systemm A, B, X, AX, BX.
Bank of AX initially between different unsaturated fluids, upstream fluid rich in B
$K_{AX} = 0.01$, $K_{BX} = 0.02$, at four times t

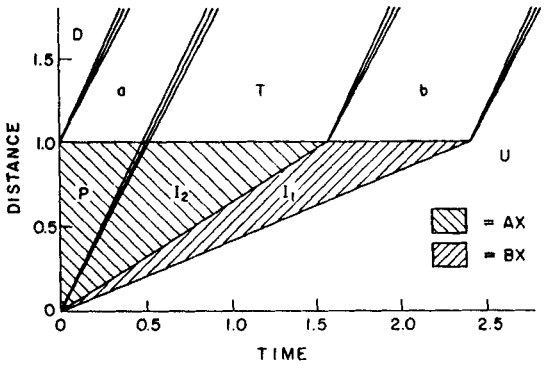

Figure 14. Distance-time diagram for sample case.
Conditions as in Figure 13; $u^o = 2.0$; initial AX bank at $0 \le z \le 1.0$
Indifferent waves are shown with arbitrary slight spreading

As the distance-time diagram shows, the first interference to occur is that of the fast wave I_2P with the standing wave Pa, namely, when fluid saturated with respect to BX reaches the downstream end of the AX bank. The noncoherence arising when this happens is between I_2 and a. With reference to the path diagram we see that this noncoherent wave will generate two new coherent waves: I_2T, a standing wave, and Ta, a wave with fluid velocity (route along paths in sequence of increasing wave velocities). The route now is DI_1I_2TaD. Even after this interference, no AX is precipitated downstream of the bank, but the fluid emerging from the latter now is saturated with respect to BX also (composition T). It displaces at fluid velocity the fluid that emerged earlier, a.

The next interference is between the shock I_1I_2 and the standing wave I_2T and occurs when all AX has been dissolved. The noncoherence arising is between I_2 and T and, as the path diagram shows, generates a standing wave I_1b and a fluid-velocity wave bT. Now the route is UI_1bTaD. BX keeps being dissolved at the upstream end of its bank, but is no longer precipitated at the downstream end. Fluid b emerging from the BX bank is saturated with respect to BX but not AX and displaces the earlier fluid T at fluid velocity.

Finally, the shock UI_1 interferes with the standing wave I_1b, when all BX has been dissolved. The standing wave is swallowed up and the route now is $UbTaD$, with four indifferent waves, all at fluid velocity. Precipitate is no longer present, and none will form again. As dissipation causes the indifferent waves to spread, they will eventually merge into a single, diffuse composition variation that spreads out over increasing distances and approaches, but never reaches, the straight-line route UD.

Nontrivial facets are that BX precipitates upstream of AX (if fluid U is rich enough in B), that the precipitates never overlap, that no precipitation of either AX or BX occurs downstream of the initial bank, and that the fluid emerging at this point is saturated with respect first to AX alone, then to both AX and BX, then to BX alone.

Extension to Systems with Additional, Nonprecipitating Species

The presence of additional, nonprecipitating species, k, adds a dimension to the phase and composition-path diagrams but presents no difficulties. Since $d\bar{C}_k = 0$ under all conditions (no precipitate contains k), any concentration variation of any such species is always propagated at fluid velocity. Accordingly, any

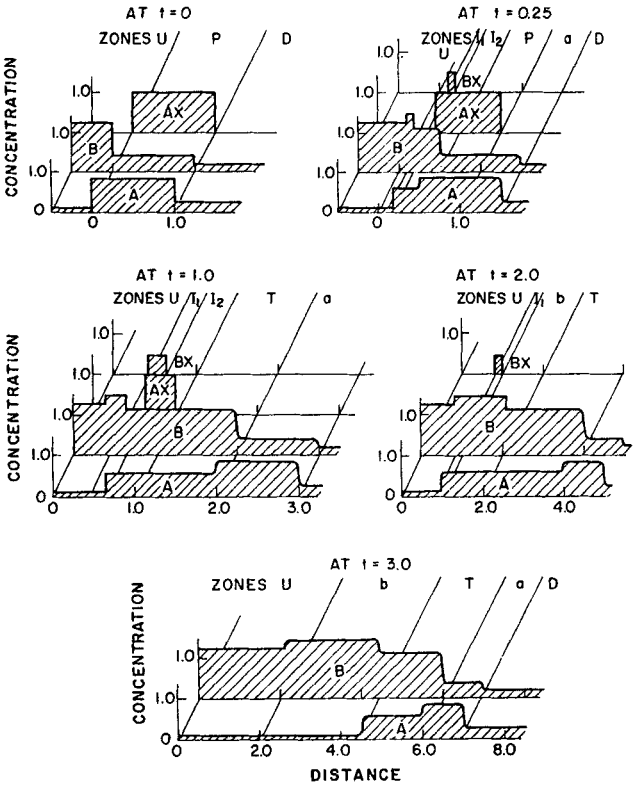

Figure 15. Transient composition profiles for sample case.
Conditions as in Figures 13 and 14

such variation can occur exclusively across a last, fluid-velocity wave of the pattern. This wave will have composition D on the downstream side. The only problem is to determine the composition on its upstream side. How this can be done becomes apparent once the path grids of these systems are understood.

Regardless of whether the additional species is an ion or a neutral molecule, the phase diagrams and path grids have the following properties, Figures 16 to 18:

Topologically, the no-precipitate, AX, BX, and $AX + BX$ regions are four blocks, each in contact with all others along one common curve (the triple curve) and extending without limit in the direction of the k axis. In Figures 16 to 18 these blocks have been moved apart for clarity.

Within the AX (or BX) region, lines parallel to the A (or B) axis correspond to variations in precipitate but not fluid-phase concentrations and thus are paths of standing waves (any standing wave is, of course, automatically coherent). Surfaces parallel to the border of the region with the no-precipitate region correspond to variations in fluid-phase but not precipitate concentrations. Any such variation thus is a coherent fluid-velocity wave: the surfaces are coherent and pathless.

In the $AX + BX$ region, any variation on a plane of constant C_k involves a variation of precipitate but not fluid-phase concentrations and so corresponds to a standing wave; these planes are coherent and pathless. Curves parallel to the triple curve (along which the four regions are in contact) involve variations of fluid-phase but not precipitate concentrations and thus are paths of coherent, fluid-velocity waves.

The simplest system of this type is A, B, M, X, AX, BX, with a neutral additional species M, Figure 16. Equations 6, 7, and 9 remain valid regardless of the value of C_M, so that the path grids on all planes of constant C_M are identical with that for the system without M, shown in Figure 2. The pathless surfaces in the AX and BX regions are curved, but parallel to the M axis. The paths in the $AX + BX$ region are straight and also parallel to the M axis.

In the system A, B, C, X, AX, BX, Figure 17, the additional ion C enters into the charge balance, and Eq. 6 must be replaced by

$$C_A + C_B + C_C = C_X \tag{25}$$

while Eqs. 7 and 9 remain valid. The border of the AX region with the no-precipitate region, calculated from Eqs. 6 and 25, is now given by

$$\tilde{C}_B = C_B = K_{AX}/\tilde{C}_A - \tilde{C}_A - C_C \tag{26}$$

For the BX region, indices A and B in this equation must be interchanged. The triple curve, which must meet both Eqs. 25 and 26, is given by

$$\tilde{C}_A^T = 2K_{AX}/[(\bar{C}_B^2 + 4K_{AX} + 4K_{BX})^{1/2} + C_C] \tag{27}$$

$$\tilde{C}_B^T = 2K_{BX}/[(\bar{C}_B^2 + 4K_{AX} + 4K_{BX})^{1/2} + C_C] \tag{28}$$

In the path diagram, the coherent surfaces in the AX and BX regions (parallel to the respective borders) are no longer parallel to the M axis, and the paths in the $AX + BX$ region (parallel to the triple curve) are curved.

For the system A, B, X, Y, AX, BX, Figure 18, the same equations apply with C_C replaced by $-C_Y$, and the properties of the phase diagram and path grid are analogous. Note that Figure 18 omits from the no-precipitate region a tetrahedral zone adjacent to the M axis; this zone corresponds to negative concentrations of X and so has no physical reality.

Route construction is now simple. The route on the plane $C_k = C_k^U$ is constructed by the same rules as for systems without k, and with an end point D' on that plane placed as follows:

- If D is in the no-precipitate region, place D' anywhere in the region on the plane $C_k = C_k^U$

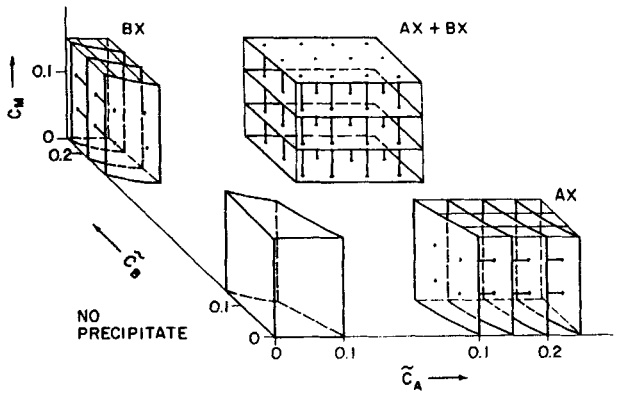

Figure 16. Phase diagram and composition paths, system A, B, M, X, AX, BX.
$K_{AX} = 0.01$; $K_{BX} = 0.2$
Planes of constant C_M (with path grids) and coherent surfaces of constant precipitate concentration are shown

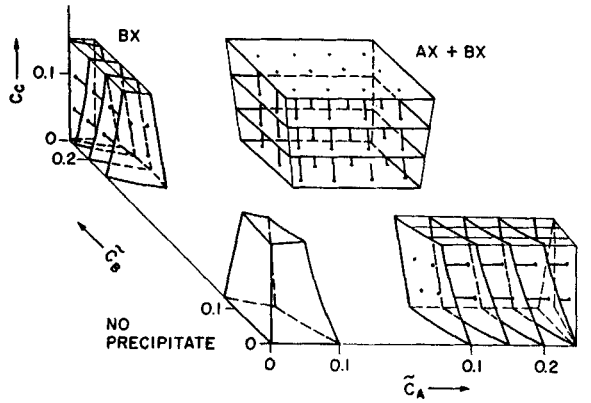

Figure 17. Phase diagram and composition paths, system *A, B, C, X, AX, BX.*

$K_{AX} = 0.01$; $K_{BX} = 0.02$

Planes of constant C_C (with path grids) and coherent surfaces of constant precipitate concentration are shown

- If D is in the AX or BX region, place D' anywhere on the intersection of the coherent surface containing D with the plane $C_k = C_k^U$
- If D is in the $AX + BX$ region, place D' on the intersection of the path through D with the plane $C_k = C_k^U$

To obtain the actual route, one replaces the last segment (to D') with one leading, instead, out of the plane $C_k = C_k^U$ to D.

For clarity, the description above was formulated for a single additional nonprecipitating species. However, since all nonprecipitating species of equal charge (or no charge) behave alike in the present context, species M, C, and Y can be viewed as lumped, representing any number of actual species of respective charge. Moreover, the extension to systems A, B, C, M, X, Y, AX, BX with nonprecipitating species of different charges, not discussed here, is straightforward in that, again, the entire route except for the last, fastest wave is on the hyperplane $C_k = C_k^U (k = C, M, Y)$.

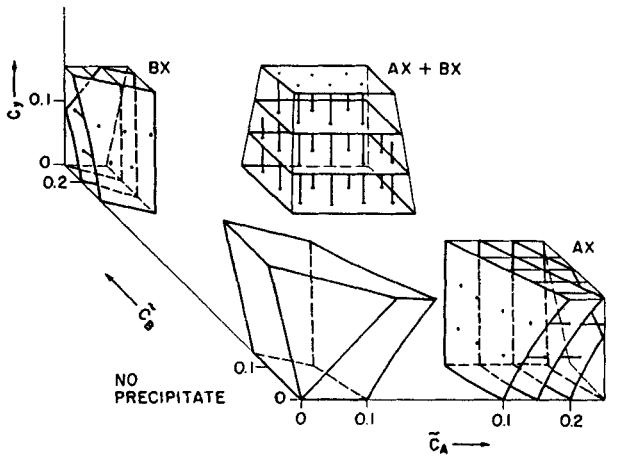

Figure 18. Phase diagram and composition paths, system *A, B, X, Y, AX, BX.*

$K_{AX} = 0.01$; $K_{BX} = 0.02$

Planes of constant C_Y (with path grids) and coherent surfaces of constant precipitate concentration are shown

Tetrahedral segment "missing" from no-precipitate region would correspond to negative concentrations of X

Discussion

The presentation has demonstrated that the concepts of multicomponent chromatography can be applied to precipitation/dissolution waves although no continuous and differentiable relations between fluid- and solid-phase concentrations exist. The new facets introduced by this complication are the occurrence of standing waves and, in the composition space, surfaces or hypersurfaces on which all variations are coherent. This is not a new phenomenon, however, as the same situation pertains in multiphase displacement in porous media (Helfferich, 1981; Hirasaki, 1981), where fluid phases become trapped if occupying less than some critical fractional phase volume.

Of greatest interest, of course, is a comparison with Bryant's theory. Most but not all of Bryant's results and conclusions are borne out at this stage. His covering postulate of invariant solid identities is no longer needed, as is not surprising since Bryant himself notes that it is essentially a consequence of coherence. His postulated downstream equilibrium condition, according to which fluid emerging from a bank containing a precipitate is saturated with respect to that precipitate, regardless of presence of other species and precipitates—an eminently plausible assumption to start with—appears as a simple consequence of a contiguous composition route. Perhaps more important, the approach taken here is much simpler than his construction of a solution function or the alternative trial-and-error procedure to locate the proper sequence of precipitates. At least in the relatively simple systems discussed here, the sequence necessarily follows from the rules for construction of coherent composition routes (e.g., see case 8 of the system A, B, X, AX, BX) and can be expressed in terms of simple geometric or algebraic criteria. Admittedly, work remains to be done to formulate these criteria for systems of greater complexity, but the capability to do so in principle cannot be questioned. The approach here also obviates the need for relatively laborious calculations with dissipation, needed in Bryant's theory in some cases to remove ambiguities in the construction of the solution function. Moreover, in many cases simple graphical procedures can replace calculations. An additional advantage is that the composition route diagrams make it much easier to visualize the behavior systems at a glance, to understand cause and effect, and to make qualitative predictions with little or no calculation. Perhaps the greatest advantage is that the approach taken here is applicable in principle to non-Riemann problems, for example, with one or several gradual starting variations, a capability which an approach based exclusively on Riemann invariants lacks.

Bryant arrived at several important conclusions that are fully confirmed here, essentially justifying his postulates. Waves under all conditions are standing waves, shocks slower than the fluid, or indifferent waves of fluid velocity (Bryant calls the last shocks, too, but this seems to be merely a matter of semantics). Standing waves involve variations of precipitate concentrations only; fluid-velocity waves, of fluid-phase concentrations only. Concentration variations of nonprecipitating species (called tracers by Bryant) always travel at fluid velocity. No precipitation-only waves can exist; that is, for a precipitate to form anywhere, another must be dissolved.

Some of Bryant's conclusions, however, have not or not yet been confirmed by the present approach. First, contrary to Bryant, more than one precipitate can completely dissolve at the same wave. An example is case 10 of the system A, B, X, AX, BX, where this occurs if U, T, and D are on the same straight

line. However, such behavior is limited to special, degenerate cases. Second, the simple systems studied here do not involve multiple shocks consisting of several successive discontinuities and partially violating the downstream equilibrium condition. Such multiple shocks were identified by Bryant in systems with at least four solids with common ions (e.g., *A*, *B*, *X*, *Y*, *AX*, *BX*, *AY*, *BY*) and appear established beyond doubt by brute-force numerical finite-difference simulations not involving any special premises (R. S. Schechter, personal communication, 1988). How such shocks will become manifest in the approach taken here and affect its procedures remains to be established.

Acknowledgment

This work was stimulated by an excellent presentation of the problem and its practical significance, given by R. S. Schechter at the ACS Symposium on Separation Science and Technology in Denver in April 1987. I also wish to thank Dr. Schechter for providing an advance copy of Bryant's thesis and clarifying many questions in lengthy discussions, as well as Dr. Bryant for a detailed critique of this manuscript.

Notation

C_i = fluid-phase concentration of i, per unit fluid volume, mol · V^{-1}
$\bar{C}_i$ = solid-phase concentration of i (total of i in any precipitates), per unit volume of fluid, mol · V^{-1}
$\tilde{C}_i \equiv \bar{C}_i + C_i$, overall concentration of i, mol · V^{-1}
K_{ij} = solubility product of precipitate ij, $mol^2 \cdot V^{-2}$
J_i = flux of i, mol · $l^{-2} \cdot t^{-1}$
l = length
t = time
u^o = linear velocity of fluid, $l \cdot t^{-1}$
u_x = linear wave velocity of dependent variable x, $l \cdot t^{-1}$
$u_{\Delta x}$ = linear velocity of shock or step Δx, $l \cdot t^{-1}$
z = space coordinate in flow direction, l
λ = velocity eigenvalue, Eq. 4, $l \cdot t^{-1}$
Λ = coherent step velocity, Eq. 5, $l \cdot t^{-1}$

Subscripts (species)

A, B, C = species of one charge sign
i, j = any precipitating species
k = any nonprecipitating species
M = uncharged species
X, Y = species of opposite charge sign

Superscripts (compositions)

a = composition at entry of route into AX from no-precipitate region
b = composition at entry of route into BX from no-precipitate region
D = composition downstream of starting variation
I, I_1, I_2 = compositions of intermediate zones in wave patterns
P = starting composition of AX bank in sample case
T = composition at triple point in system A, B, X, AX, BX
U = composition upstream of starting variation

Literature Cited

Adler, H. H., "Concepts of Uranium-Ore Formation in Reducing Environments in Sandstones and Other Sedments," *Proc. Symp. on Formation of Uranium Ore Deposits,* Int. Atomic Energy Agency, Athens, Greece (May, 1974).

Aris, R., and N. R. Amundson, *Mathematical Methods in Chemical Engineering,* **II,** Prentice-Hall, Englewood Cliffs, NJ (1973).

Bartlett, R., and B. James, "Behavior of Chromium in Soils. III: Oxidation," *J. Environ. Quality,* **8,** 31 (1979).

Bartlett, R. J., and J. M. Kimble, "Behavior of Chromium in Soils. I: Trivalent Forms," *J. Environ. Qual.,* **5,** 379 (1974).

Bryant, S. L., "Wave Behavior in Reactive Flow Through Permeable Media," Ph.D. Thesis, Univ. Texas, Austin (1986).

Bryant, S. L., R. S. Schechter, and L. W. Lake, "Interactions of Precipitation/Dissolution Waves and Ion Exchange in Flow Through Permeable Media," *AIChE J.,* **32,** 751 (1986).

———, "Mineral Sequences in Precipitation/Dissolution Waves," *AIChE J.,* **33,** 1271 (1987).

Dria, M. A., S. L. Bryant, R. S. Schechter, and L. W. Lake, "Interacting Precipitation/Dissolution Waves: The Movement of Inorganic Contaminants in Groundwater," *Water Resources Res.,* **23,** 2076 (1987).

Galloway, W. E., "Epigenetic Zonation and Fluid Flow History of Uranim-Bearing Fluvial Aquifer Systems, South Texas Uranium Province," Bur. Economic Geol., Univ. Texas, Austin (1982).

Gao, H. W., H. Y. Sohn, and M. E. Wadworth, "A Mathematical Model for the *in situ* Leaching of Primary Copper Ore," *Interfacing Technologies in Solution Mining,* W. J. Schlitt, J. B. Hiskey, eds., Proc. 2nd SME/SPE Int. Solution Mining Symp., Denver (Nov., 1981).

Griffin, R. A., A. K. Au, and R. R. Frost, "Effect of pH on Adsorption of Chromium from Landfill-Leachate by Clay Minerals," *J. Environ. Sci. Health,* **A12,** 431 (1977).

Hahne, H. C. H., and W. Kroontje, "Significance of pH and Chloride Concentration on Behavior of Heavy Metal Pollutants: Mercury (II), Cadmium (II), Zinc (II), and Lead (II)," J. Environ. Qual., **2,** 444 (1973).

Helfferich, F., "Chromatographic Behavior of Interfering Solutes," *Adsorption from Aqueous Solution,* R. F. Gould, ed., Am. Chem. Soc., 30 (1968).

———, "Theory of Multicomponent, Multiphase Displacement in Porous Media," *SPE J.,* **21,** 51 (1981).

———, "Conceptual View of Column Behavior in Multicomponent Adsorption or Ion-Exchange Systems," *AIChE Symp. Ser.,* **80**(233), 1 (1984).

———, "Multicompnoent Wave Propagation: Attainment of Coherence from Arbitrary Starting Conditions," *Chem. Eng. Commun.,* **44,** 275 (1986).

———, "Coherence: Power and Challenge of a New Concept," *New Directions in Adsorption Technology,* G. Keller, ed., Butterworth, (accepted for pub., 1988).

Helfferich, F. G., and G. Klein, *Multicomponent Chromatography,* Dekker, New York (1970; available from University Microfilms, Ann Arbor, MI, #2050382).

Hirasaki, G. J., "Application of the Theory of Multicomponent, Multiphase Displacement to Three-Component, Two-Phase Surfactant Flooding," *SPE J.,* **21,** 191 (1981).

Jeffrey, A., *Quasilinear Hyperbolic Systems and Waves,* Pitman, London (1976).

Khalid, R. A., "Chemical Mobility of Cadmium in Sediment-Water Systems," *Cadmium in Environment,* J. O. Nriagu, ed., *I: Ecological Cycling,* Wiley, New York, 258 (1980).

Klein, G., "Fixed-Bed Ion Exchange with Formation or Dissolution of Precipitate," *Ion Exchange: Science and Technology,* R. Rodrigues, ed., Nijhoff, Dordrecht, 199 (1986).

Korzhinskii, D. S., *Theory of Metasomatic Zoning,* Oxford, London (1970).

Miller, C. W., and L. V. Benson, "Simulation of Solute Transport in a Chemically Reactive Heterogeneous System: Model Development and Application," *Water Resources Res.,* **19,** 389 (1983).

Rhee, H-K., and N. R. Amundson, "An Analysis of an Adiabatic Adsorption Column," *Chem. Eng. J.,* **1,** 241 (1970).

Stohs, M., "A Study of Metal Ion Migration in Soils from Drilling Mud Pit Discharges," M.S. Thesis, Univ. Texas, Austin (1986).

Tatom, T. A., R. S. Schechter, and L. W. Lake, "Factors Influencing the *in situ* Acid Leaching of Uranium Ores," *Interfacing Technologies in Solution Mining,* W. J. Schlitt, J. B. Hiskey, eds., Proc. 2nd Int. Solution Mining Symp., Denver (Nov., 1981).

Walsh, M. P., S. L. Bryant, L. W. Lake, and R. S. Schechter, "Precipitation and Dissolution of Solids Attending Flow Through Porous Media," *AIChE J.,* **30,** 317 (1984).

Manuscript received Apr. 12, 1988, and revision received Aug. 31, 1988.